ELSEVIER

Biochemical Pharmacology 63 (2002) 1653–1662

Biochemical Pharmacology

Intercalation of imidazoacridinones to DNA and its relevance to cytotoxic and antitumor activity☆

Jarosław Dzięgielewski[a,1], Bartłomiej Ślusarski[a], Antoni Konitz[b,c], Andrzej Składanowski[a], Jerzy Konopa[a,*]

[a]*Department of Pharmaceutical Technology and Biochemistry, Technical University of Gdańsk, Narutowicza 11/12, 80-952 Gdańsk, Poland*
[b]*Department of Inorganic Chemistry, Technical University of Gdańsk, Gdańsk, Poland*
[c]*Department of Chemistry, University of Gdańsk, Gdańsk, Poland*

Received 28 September 2001; accepted 12 February 2002

Abstract

Imidazoacridinones (IA) are a class of antitumor agents which includes C-1311, an interesting drug in clinical trials. This study investigated the mechanism of IA binding to DNA for a series of 13 analogs that differ in their cytotoxic potency. Using C-1311 as a model compound, crystallographic, spectroscopic and biochemical techniques were employed to characterize drug–DNA interactions. X-ray crystallographic analysis revealed a planar structure of imidazoacridinone core that is capable of intercalative DNA binding. Accordingly, C-1311 binding to DNA followed 'classical' pattern observed for intercalation, as proved by the DNA topoisomerase I—unwinding experiments, with relatively weak binding affinity ($K_i = 1.2 \times 10^5\ M^{-1}$), and the binding site size of 2.4 bp. Other IA also bound to DNA with the binding affinity in the range of $10^5\ M^{-1}$ and binding site size of 2–3 bp, suggesting a prevalence of the intercalative mechanism, similar to C-1311. Considerable DNA binding affinity was displayed by all the highly cytotoxic derivatives. However, none of the analyzed drug–DNA binding parameters was significantly correlated with IA biological activities such as cell growth, DNA and RNA synthesis inhibition, or tumor growth inhibition, which suggests that the IA ability to non-covalently bind to DNA is not crucial for their biological activity. These results show that the ability to intercalate into DNA is a prominent attribute of IA, although factors other than intercalative binding seem to be required for the biological activities of IA drugs.

Keywords: C-1311; DNA intercalation; Structure–activity relationship; Crystal structure; Imidazoacridinones

1. Introduction

IA (see Table 1 for structures) are a group of antitumor compounds synthesized in our laboratory [1,2]. IA are cytotoxic *in vitro* against various human and murine cell lines and exhibit *in vivo* activity against leukemia P388, melanoma B16, ascites colon 26 adenocarcinoma, colon 38 adenocarcinoma, MAC29 colon carcinoma and HT29 colon in mice [3,4]. The most promising analog, C-1311 (for review see [5]), has been selected for the clinical development by European Organization for Research and Treatment of Cancer (EORTC).

Despite the advanced stage in clinical development, the knowledge of the mechanism of action of IA is limited. C-1311 was shown to accumulate in the cell nucleus [4,6,7], to inhibit cellular nucleic acids synthesis [4,8], and to trap topoisomerase II cleavage complexes [6]. Cell growth inhibition by IA was accompanied by the induction of G_2 block of the cell cycle [9] followed by apoptosis [7]. This pattern suggested that cellular DNA might be a target for the IA drugs. Given the structural resemblance of IA to other anticancer agents, such as anthracenediones, that are known to bind to DNA, it was possible that DNA binding may play a role also in the case of IA.

☆ Preliminary account of these studies has been presented at 9th EORTC-NCI Symposium on New Drug Development, Amsterdam, The Netherlands, 1996.

* Corresponding author. Tel.: +48-58-347-15-16; fax: +48-58-347-15-16.
E-mail address: konopa@altis.chem.pg.gda.pl (J. Konopa).
[1] Present address: Department of Pharmacology and Therapeutics, Roswell Park Cancer Institute, Buffalo, NY, USA.

Abbreviations: ctDNA, calf thymus DNA; EC_{50}, concentration inhibiting cell growth by 50%; Hepes, 4-(2-hydroxyethyl)-1-piperazine-ethanesulfonic acid; IA, imidazoacridinones; pEC_{50}, negative log from EC_{50} value; PBS, phosphate buffered saline; SDS, sodium dodecyl sulfate; TCA, trichloroacetic acid.

0006-2952/02/$ – see front matter
PII: S0006-2952(02)00916-4

Table 1
Chemical structures and biological activities of studied imidazoacridinones

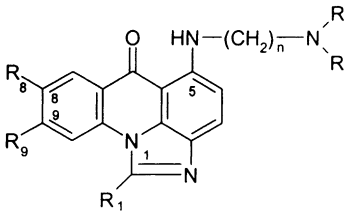

Compound	Chemical structure					Biological activity[a]		
	R	*n*	R_1	R_8	R_9	L1210 *in vitro*	P388 leukemia in mice	
						EC_{50} (μM)	OD (mg kg^{-1})	*T/C* (%)
C-1176	CH_3	2	H	H	H	1.19	150	190
C-1212	CH_3	3	H	H	H	1.95	100	125
C-1263	CH_3	2	H	OH	H	0.051	12.5	210
C-1266	CH_3	5	H	H	H	3.03	100	110
C-1310	CH_2CH_3	2	CH_3	OH	H	0.25	50	285
C-1311	CH_2CH_3	2	H	OH	H	0.031	5	193
C-1330	CH_2CH_3	2	H	OCH_3	H	1.78	90	196
C-1371	CH_3	3	H	OH	H	0.034	5	193
C-1415	CH_2CH_3	2	H	H	H	1.72	175	155
C-1419	CH_2CH_3	2	H	H	OH	1.96	50	127
C-1492	CH_3	5	H	OH	H	1.12	75	185
C-1554	CH_2CH_3	2	H	CH_3	H	1.42	200	120
C-1558	CH_2CH_3	2	H	*t*-Butyl	H	3.44	25	110

[a] Data were taken from Cholody *et al*. [1,2]. OD and *T/C* are the optimal dose and the median survival time of treated animals divided by median survival of controls. The EC_{50} is the concentration of the compound inhibiting growth of L1210 cells by 50%.

Preliminary report of this study [8] and the data published by others [4,7] suggested indeed that IA drugs are capable of binding to DNA. The nature of these interactions and their relevance to cytotoxic and antitumor properties of IA compounds remains unknown. Since targeting cellular DNA is likely to be significant for the cytotoxic and antitumor properties of IA, it became necessary to evaluate in a quantitative and systematic way various aspects of drug–DNA interactions using a coherent set of analogs displaying divergent biological activities.

In this study, we verified by X-ray crystallography that C-1311 contains planar polycyclic aromatic ring system required for the intercalation into DNA. Intercalative DNA binding has been demonstrated for C-1311 by several approaches. Analysis of several IA analogs of C-1311 showed that the ability to interact with DNA is a common attribute of cytotoxic IA drugs. The differences in DNA binding properties, however, do not fully account for the diverse biological activities of the IA drugs studied.

2. Materials and methods

2.1. Chemicals

IA were synthesized and purified as described earlier [1,2]. Stock solutions (1 mM) were prepared in water and stored at −20°. The RPMI-1640 medium, fetal calf serum, simian virus (SV40) supercoiled DNA and human topoisomerase I were obtained from Life Technologies (Paisley, UK). Methyl-[^{3}H]-thymidine, 5-[^{3}H]-uridine were from Amersham Ltd. (Piscataway, NJ, USA). Calf thymus DNA (ctDNA) (type II) from Sigma (St. Louis, MO, USA) was used after sonication. The concentrations of DNA solutions were expressed in terms of moles of base pairs per liter, using molar extinction coefficient of $\varepsilon_{260} = 13{,}200\ M^{-1}\ cm^{-1}$. The drug–DNA interaction experiments were conducted in HS buffer (5 mM 4-(2-hydroxyethyl)-1-piperazine-ethanesulfonic acid (Hepes), 150 mM NaCl, pH 7.0), TE buffer (10 mM Tris–HCl, 0.1 mM EDTA, pH 7.4) or topoisomerase reaction buffer (100 mM Tris–HCl, 50 mM KCl, 5 mM $MgCl_2$, 0.1 mM EDTA, pH 7.5).

2.2. X-ray structure analysis

Compound C-1311 (C-1311 × 2HCl × $3H_2O$) crystallizes in the monoclinic space group $P2_1/c$ with the unit cell parameters: $a = 5.270(3)$, $b = 13.299(3)$, $c = 12.152(2)$ Å, $\beta = 109.91(3)$, $V = 2320.3(8)$ Å^3, $Z = 4$. The intensities of reflections were measured with Kuma KM-4 diffractometer (Mo Kα radiation, graphite monochromator, $2\theta_{max} = 60°$) for a crystal with dimensions 0.3 mm × 0.3 mm × 0.6 mm. In total, 5115 independent reflections were collected, of which 2874 had $I > 2\sigma(I)$. The structure was solved by direct methods with the program SHELXS-86 [10].

Table 2
Crystallographic data and structure refinement for C-1311

Parameter	Value
Empirical formula	$C_{20}H_{30}Cl_2N_4O_5$
Molecular weight	477.38
Temperature (K)	293(2)
Wavelength (Å)	0.71073
Unit cell dimensions	$a = 15.270(3)$ Å, $\alpha = 90^\circ$ $b = 13.299(3)$ Å, $\beta = 109.91(3)^\circ$ $c = 12.152(2)$ Å, $\gamma = 90^\circ$
Volume (Å^3)	2320.3(8)
Z	4
Calculated density (mg m^{-3})	1.367
Absorption coefficient (mm^{-1})	0.318
$F(0\,0\,0)$	1008
Theta (θ) range for data collection ($^\circ$)	1.42–30.05
Index ranges	$-20 \le h \le 0$, $-16 \le k \le 0$, $-13 \le l \le 16$
Reflections collected/unique	5215/5115 [R(int) = 0.0358]
Completeness to $2\theta = 30.05$	72.2%
Refinement method	Full-matrix least-squares on F^2
Data/restraints/parameters	5115/10/309
Goodness-of-fit on F^2	1.042
Final R indices ($I > 2\sigma(I)$)	$R_1 = 0.0664$, $wR_2 = 0.1509$
R indices (all data)	$R_1 = 0.1293$, $wR_2 = 0.1834$
Extinction coefficient	0.0025(6)
Largest diff. peak and hole (Å^{-3})	0.390 and −0.254

Full matrix least-square refinement was carried out on F^2 with SHELXL-97 [11]. All hydrogen atoms were found in different Fourier maps and were refined in idealized positions with temperature factors 1.2 times of U_{eq} of the preceding atoms, except for hydrogen atoms of two methyl groups for which the common isotropic temperature factor for hydrogen atoms was refined. Final values of R indices for all data were: $R_1 = 0.0664$, $wR_2 = 0.1509$ for $I > 2\sigma(I)$ and $R_1 = 0.1293$, $wR_2 = 0.1834$. Maximum residual electron density was 0.32 e Å^{-3} (0.39 at the chlorine anions). A summary of crystallographic data and structure refinement is given in Table 2.

2.3. Self-aggregation studies

Absorption spectra were recorded with Perkin-Elmer LambdaBio UV–VIS spectrophotometer at room temperature (20°) using a range of drug concentrations (1–200 μM) in HS buffer. The molar extinction coefficients of the monomer (ε_M) and dimer (ε_D) forms of the drugs, as well as dimerization constants (K_D) were calculated according to the method of Schwarz [12] as previously described elsewhere [13]. The monomer extinction coefficient was estimated by extrapolation of the apparent extinction coefficient to infinite dilution of a given compound, then based on the additivity of the absorption of monomer and dimer in the mixture, the dimer extinction coefficient and dimerization constant were found.

2.4. Spectrophotometric titration

Spectral titration measurements were carried out at room temperature (20°) using ctDNA (type II) in standard HS buffer. Binding was monitored spectrophotometrically within the IA absorption region (300–550 nm) with Perkin-Elmer LambdaBio UV–VIS spectrophotometer. One milliliter aliquot of DNA (100–500 μM) dissolved in HS buffer was mixed with a small volume (2–20 μL) of compound stock solution (0.5–1 mM) in a cuvette, incubated for 10 min, and then the absorption spectra were recorded.

2.5. Fluorimetric titration

Fluorescence assays were performed at 20° in a 1 cm quartz cuvette with a Perkin-Elmer LS-5B luminescence spectrometer. Slit widths of 2.5 nm were typically used with extinction monochromator set between 400 and 430 nm for different compounds as specified in Table 3. The binding isotherms were calculated from fluorescence

Table 3
Absorption and fluorescence spectra of imidazoacridinones and their complexes with DNA in HS buffer (pH 7) at 20°

Compound	Absorption λ_{max} (nm)[a]			Fluorescence λ_{max} (nm)			
	Monomer	Dimer	Complex	Ex compound	Em compound	Ex complex	Em complex
C-1176	418	425	428	418	521	418	508
C-1212	429	432	435	429	528	436	511
C-1263	420	432	423	416	524	419	507
C-1266	434	437	444	434	532	444	517
C-1310	428	438	437	428	534	437	522
C-1311	420	432	429	419	524	426	506
C-1330	423	431	428	420	524	433	506
C-1371	429	440	438	436	533	438	515
C-1415	420	424	424	417	520	419	504
C-1419	409	417	420	409	483	414	487
C-1492	439	442	444	442	534	443	518
C-1554	420	426	421	415	516	421	498
C-1558	421	422	420	417	518	418	484

[a] λ_{max} is the wavelength of absorbance or fluorescence maximum. Ex: fluorescence excitation spectrum; Em: fluorescence emission spectrum; complex: drug:DNA complex. All details are described in Section 2.

data collected over a wide range of compound to DNA ratios [14]. Each binding determination consisted of a minimum of 20 different DNA concentrations. The cuvettes contained 2 μM drug, HS buffer, and ctDNA. The concentration of free ligand was calculated from equation

$$C_F = \frac{C_T((I/I_0) - P)}{1 - P}$$

where C_T and C_F are the total and free compound concentrations, and I_0 and I are the fluorescence intensities of free drug and the sample. P was obtained from the extrapolation of plot I/I_0 vs. $1/C_{DNA}$ to zero. The intrinsic binding constants (K_i) and the exclusion parameter (n) were determined according to the neighbor exclusion model of ligand–polymer interaction [15] using the McGhee and von Hippel equation

$$\frac{v}{C_F} = K_i(1 - nv)\left[\frac{1 - nv}{1 - (n-1)v}\right]^{n-1}$$

where n is the number of moles of a compound bound per DNA base pair. A computer program for performing these calculations was kindly provided by Dr. Jan Mazerski (Technical University of Gdańsk, Poland).

2.6. DNA thermal denaturation studies

Stabilization of DNA duplexes was studied by determining melting temperatures of ctDNA in the presence of 10 μM IA in TE buffer. Compounds tested were mixed with DNA at 1:4 drug/bp ratio. Samples were heated over the range 20–95° (using a heating rate of 1° min^{-1}) and sample absorbance at 260 nm was continuously recorded in a Varian 635 UV–VIS spectrophotometer equipped with a programmable heating unit. The 'melting' temperature (T_m) was read from the plot of relative hyperchromicity vs. the temperature as the midpoint of the hyperchromic transition [16].

2.7. DNA unwinding assay

The imidazoacridinone-induced DNA unwinding was examined using DNA topoisomerase I assay [17]. Supercoiled SV40 DNA (0.4 μg) was incubated with 5 U of topoisomerase I (Life Technologies Inc.) in 30 μL topo I reaction buffer. After 5 min at 37°, a compound to be tested was added and the incubation continued for 60 min. Reactions were stopped with sodium dodecyl sulfate (SDS) and proteinase K (final concentrations 1% and 0.5 mg mL^{-1}, respectively). After an additional 15 min at 37°, the samples were extracted with phenol:chloroform:isoamyl alcohol (25:24:1) and electrophoresed overnight at 1 V cm^{-1} in 1% agarose gel using TAE buffer (40 mM Tris–acetate, 10 mM EDTA, pH 8.0). DNA bands were visualized with ethidium bromide (0.5 μg mL^{-1}) and photographed under UV.

2.8. Cell culture

L1210 murine leukemia cell line (ATCC) was used throughout these studies. The cells were routinely maintained in RPMI-1640 medium containing 5% fetal calf serum and antibiotics (100 μg mL^{-1} streptomycin, 100 U mL^{-1} penicillin), at 37° in a humidified 5% CO_2–95% air atmosphere.

2.9. Inhibition of cellular nucleic acid synthesis

Inhibition of DNA or RNA synthesis was determined as described earlier [18] based on radiolabeled precursor incorporation into trichloroacetic acid (TCA) insoluble material. The results are expressed as drug concentrations inhibiting by 50% the incorporation of [^{3}H]-thymidine and [^{3}H]-uridine, respectively.

3. Results

The imidazoacridinone derivatives examined in this study have been selected to include analogs with divergent structures, covering a range of cytotoxic and anticancer activities (Table 1). All these compounds share the same core structure of IA with two varying elements: (1) ring substitutions in the position 5, 7 or 8, and (2) diaminoalkyl side chain of variable length.

3.1. Crystal structure

A summary of crystallographic data for C-1311 and structure refinement is given in Table 2. Fig. 1 (panel A and B) shows the stereochemistry of C-1311 molecule in its crystal structure. The acridine chromophore and the imidazolo ring are planar. The diaminoalkyl side chain is perpendicular to aromatic nucleus (torsion angle C(1)–N(19)–C(20)–C(21) = −84.4°). The nitrogen N(19) and carbon C(20) bond is coplanar with the aromatic nucleus, suggesting an intramolecular hydrogen bond between N(19) and O(17).

3.2. UV–VIS absorption spectra

C-1311 shows absorbance in the range 350–500 nm (examples of C-1311 spectra in Fig. 2) with molar extinction coefficients ε_{max} in the order of 10^4 cm^{-1} M^{-1}. With the increase in drug concentration, the hypo- and bathochromic shifts in its spectrum were observed, indicative of intermolecular interactions, presumably self-aggregation. An isosbestic point was observed in the titration experiments, indicating the presence of two components in the sample, which probably correspond to a monomer and dimer. At lower drug concentrations (<5–10 μM), C-1311 seems to exist in solution mainly as the monomer, whereas a progressive dimerization is noted at higher drug

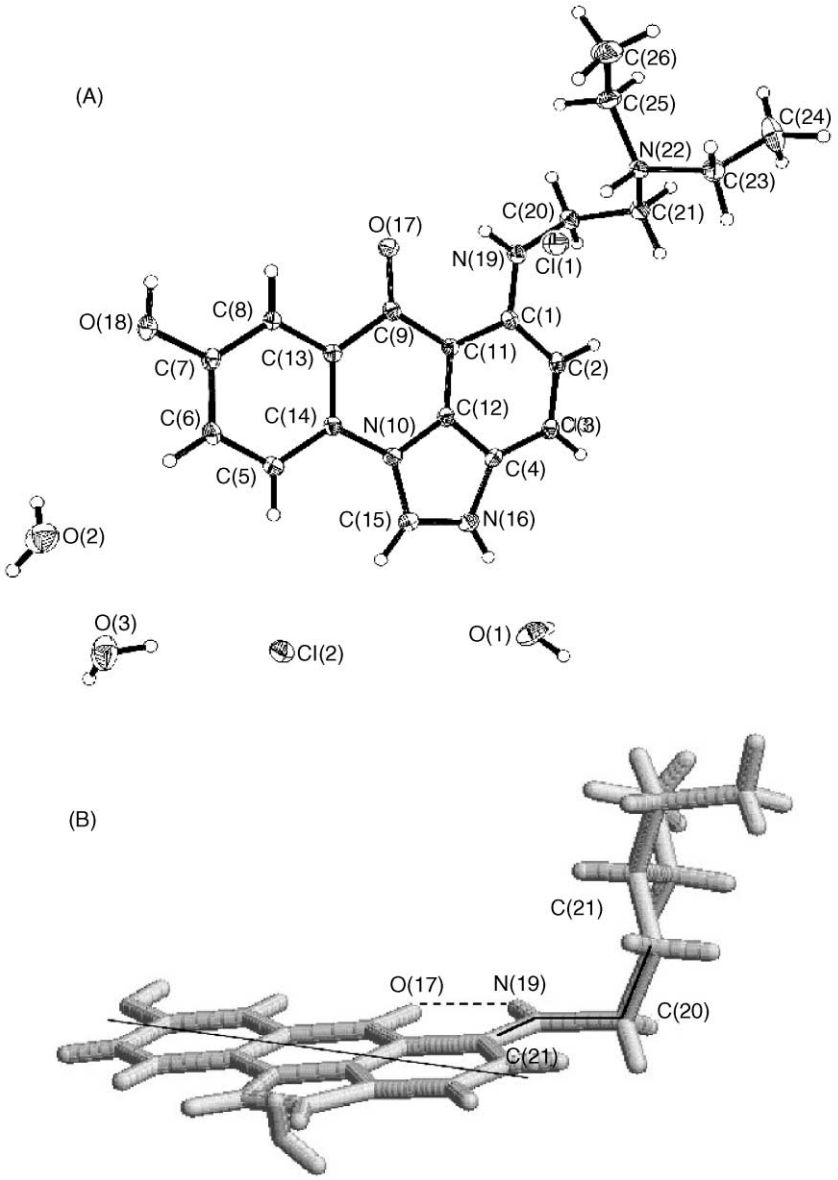

Fig. 1. Crystal structure of imidazoacridinone C-1311.

concentrations. Upon addition of ctDNA, the spectrum of monomeric form of C-1311 exhibited hypochromic (decrease in absorbance) and bathochromic effects (shift to higher wavelength), typical for interactions between π electrons of a ligand and π electrons of nucleic bases.

Absorbance spectra of other IA compounds examined in the absence and presence of DNA exhibited similar properties to those of C-1311 (for the complete spectral parameters see Table 3). Dimerization constants calculated for IA were in the order of $10^4\ M^{-1}$, and were comparable to dimerization constants shown for similar planar compounds such as anthracenediones [13,19], aza-anthracenediones [20] and ellipticines [21]. Hypochromic and bathochromic spectral shifts in the presence of DNA (Table 3) were noted for all IA compounds. These changes, however, were more profound for some compounds (e.g. C-1419, C-1176, C-1266, C-1311, C-1310, C-1371) than for the others (e.g. C-1558, C-1263, C-1554) suggesting differences in DNA affinity.

3.3. Fluorescence spectra

Spectrofluorimetric analysis was used to further characterize the selected set of compounds for their ability to interact with DNA. Fluorescent spectra of C-1311 and its complexes with DNA are given as an example in Fig. 3A and the fluorescence parameters for all the studied compounds are summarized in Table 3. All these drugs showed strong fluorescence when excited at 420–440 nm with maximum of emission at 500–540 nm. The emission consisted of a single broad band, regardless of differences in chemical structure or absorption spectra of studied compounds.

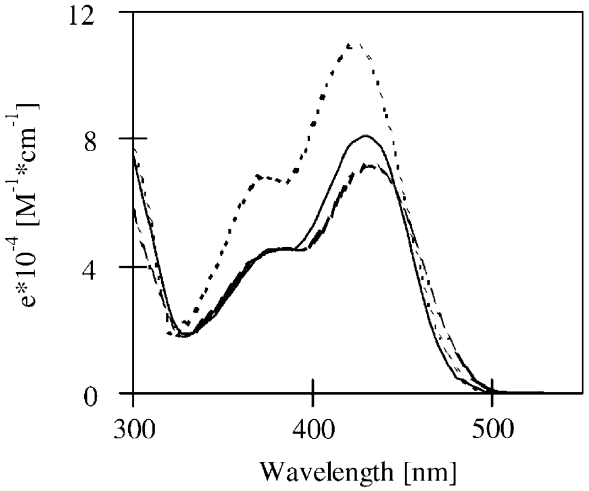

Fig. 2. Absorption spectra of C-1311 ((· · ·) monomer, (- - -) dimer, calculated as described in Section 2) and its complex with DNA (—) in HS buffer, pH 7, 20°.

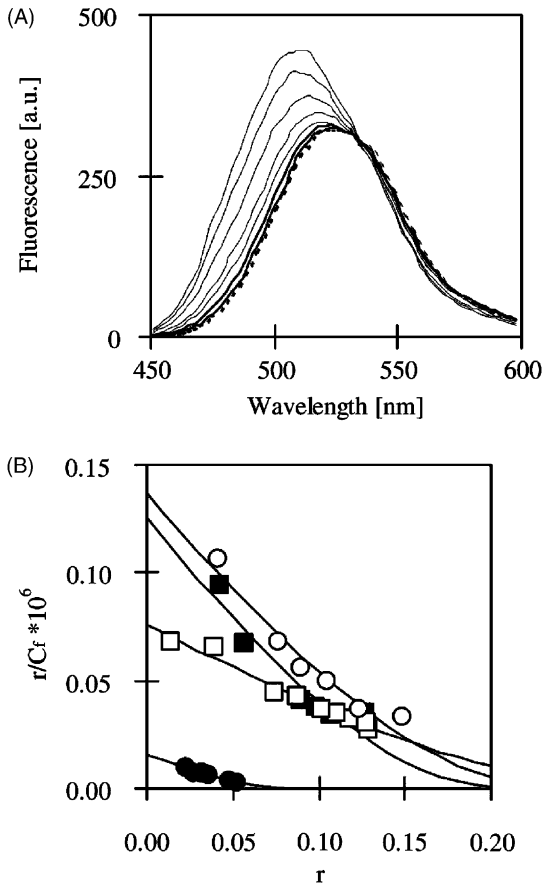

Fig. 3. Fluorescence spectral analysis of imidazoacridinones binding to DNA. (A) Fluorescence emission spectra of C-1311 (· · ·) and its complex with DNA (—) in HS buffer, pH 7 at 20°. Maxima from bottom to top correspond to increasing DNA concentration. (B) Scatchard plots illustrating the interactions of selected imidazoacridinones with DNA in HS buffer (pH 7) at 20° derived from the spectral analysis like the one for C-1311 shown in panel A. The curve represents the best fit of the McGhee–von Hippel equation to the experimental points. (■) C-1311; (□) C-1330; (○) C-1415; (●) C-1558.

Titration of IA solutions with DNA resulted in increases in emission signals and spectral shifts to shorter wavelengths for all 13 compounds, similar to the changes shown in Fig. 3A for C-1311 complexes with DNA. These changes in fluorescence spectra could be observed at quite low drug concentrations (e.g. 2 μM for C-1311) at which the majority of free drug molecules exist as monomers. This property facilitates the use of the spectrofluorimetric titration for the evaluation and quantitation of drug binding affinity. The intrinsic binding constant (K_i) and exclusion size (n) were calculated from binding isotherms obtained from fluorescence data for all thirteen IA. Representative Scatchard plots for C-1311, C-1330, C-1415 and C-1558 are shown in Fig. 3B, and the complete results are summarized in Table 4. Under ionic conditions employed (150 mM NaCl, pH 7), all the compounds examined bound to ctDNA with the affinity K_i in the order of 10^5 M^{-1} (Table 4). For all but two compounds, the exclusion size parameter ranges from 2 to 3, consistent with the intercalative mode of binding. The 8-OH substituted compounds, with the exception of C-1492, showed enhanced DNA binding compared to unsubstituted- or alkyl-substituted derivatives. C-1558, a compound with the bulky substituent (*t*-butyl) attached to acridinone moiety, displayed the lowest DNA affinity ($K_i = 0.16 \times 10^5$) and the largest exclusion size ($n = 4.6$).

3.4. DNA duplex stabilization

Thermodynamic stabilization of DNA duplexes is another binding property of potential biological significance. All the studied compounds shifted DNA melting profiles to higher temperatures when analyzed at 10 μM drug concentration (1:4 drug:DNA base pair molar ratio). The resulting melting curves were monophasic (data not shown), and the increases in DNA melting point (ΔT_m

Table 4
Parameters describing interactions of imidazoacridinones with DNA

Compound	DNA affinity		dsDNA stabilization
	$K_i \times 10^{-5}$ (M^{-1})[a]	n	ΔT_m (°)
C-1176	0.58 ± 0.03	2.1 ± 0.1	9.5 ± 0.5
C-1212	1.4	2.0 ± 0.2	11.5 ± 1
C-1263	1.2 ± 0.2	2.0 ± 0.3	12.3 ± 1
C-1266	1.0 ± 0.3	2.6 ± 0.6	9.9 ± 1
C-1310	1.31 ± 0.02	2.2 ± 0.1	15.3 ± 2
C-1311	1.2 ± 0.2	2.4 ± 0.8	13.7 ± 1
C-1330	0.75 ± 0.06	2.4 ± 0.3	11.5 ± 0.5
C-1371	1.46 ± 0.2	2.6 ± 0.3	3.5 ± 1
C-1415	1.36 ± 0.02	2.5 ± 0.6	7.2 ± 1
C-1419	1.8 ± 0.6	2.3 ± 0.2	8.3 ± 1
C-1492	0.76 ± 0.02	3.8 ± 0.2	13.1 ± 2
C-1554	1.3 ± 0.2	2.6 ± 0.8	10.5 ± 3
C-1558	0.16 ± 0.08	4.6 ± 1	2.4 ± 1

[a] K_i: intrinsic binding constant; n: neighbor exclusion size (base pairs); ΔT_m: increase in DNA melting temperature at drug to DNA 1:4 molar ratio. All details are described in Section 2.

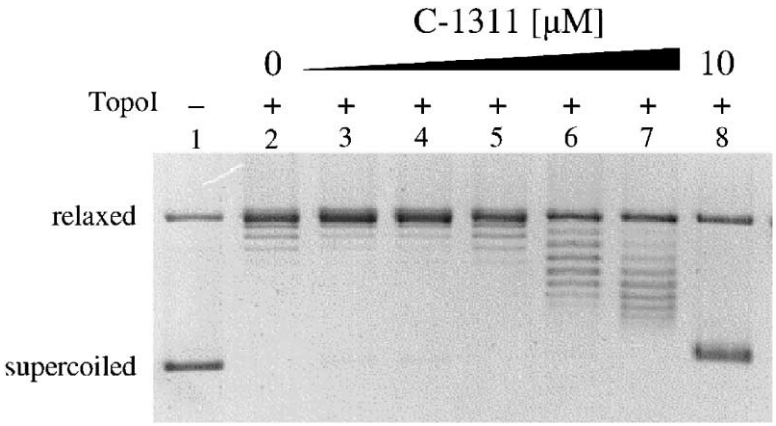

Fig. 4. The influence of C-1311 on circular DNA topology. Native supercoiled SV40 DNA (lane 1) was reacted with an excess of topoisomerase I in the absence of the drug (lane 2) or in the presence of the increasing concentrations of C-1311 (lanes 3–10) for 60 min at 37°. Reactions were stopped, samples run on 1% agarose gel in TAE buffer and DNA topoisomers were visualized after staining with ethidium bromide.

values) varied from 2 to 15°, depending on chemical structure of IA (Table 4). Derivatives with hydroxyl in position 8 (C-1263, C-1310, C-1311, and C-1492), stabilized the double-strand DNA structure most significantly. Compound C-1558, bearing *t*-butyl group in position 8, caused only marginal increase in DNA T_m of 2.4°.

3.5. DNA unwinding

Drug-induced DNA unwinding, a hallmark of interactive mode of binding, can be conveniently analyzed by topoisomerase I plasmid unwinding assay. Fig. 4 shows a representative gel electrophoresis of SV40 DNA pre-relaxed with topoisomerase I and then further incubated with C-1311 (0–10 μM) in the presence of topoisomerase I. During the reactions, the enzyme relaxes positive supercoils generated by drug-induced duplex unwinding. In this way, topoisomerase I changes DNA linking number, in a manner proportional to the magnitude of drug-induced unwinding. Following drug removal by phenol extraction, these altered linking number values result in re-winding of topoisomers from drug-treated samples, whereas control DNA remains relaxed. Under the conditions of electrophoresis, the fully relaxed DNA incubated in the absence of a drug migrates as slightly positively supercoiled [17]. Topoisomer distributions in samples treated with 0.3 and 0.6 μM C-1311 (lanes 3 and 4, respectively) are consistent with a transition to negative supercoiling that progresses further with increasing C-1311 concentrations, as reflected by the accelerated DNA migration. These characteristic patterns of topoisomer distribution provide the unequivocal evidence for the intercalative mode of C-1311 binding to DNA.

3.6. Inhibition of DNA and RNA biosynthesis induced by imidazoacridinones

IA inhibited the incorporation of precursors into DNA and RNA in L1210 cells by 50% (IC_{50} DNA and IC_{50} RNA) at concentrations ranging from 0.49 to 8.29 μM (Table 5). Preferential inhibition of DNA synthesis over RNA synthesis was clearly visible for the most cytotoxic derivatives (C-1263, C-1310, C-1311), whereas there were only slight differences between inhibition of DNA and RNA synthesis for the less active derivatives (C-1176, C-1212, C-1330, C-1419, C-1554 and C-1558).

3.7. The lack of correlation between DNA binding and biological properties of imidazoacridinones

To assess a possible contribution of DNA interaction to cellular effects of the IA drugs, we examined relationships between their cytotoxic and antitumor activities (Table 1) and DNA binding parameters (Table 4). No significant correlation could be identified between DNA affinity or duplex stabilization (expressed as K_i and ΔT_m values,

Table 5
Inhibition of the nucleic acids synthesis (precursors incorporation) in L1210 cells after 3 hr incubation with imidazoacridinones

Compound	Concentration inhibiting incorporation of precursors into L1210 tumor cells	
	IC_{50} DNA (μM)[a]	IC_{50} RNA (μM)
C-1176	4.09 ± 2.1	5.44 ± 1.1
C-1212	5.36 ± 1.9	3.50 ± 0.08
C-1263	0.81 ± 0.33	2.88 ± 0.96
C-1266	11.3 ± 2.9	19.5 ± 1.3
C-1310	1.74 ± 0.09	2.27 ± 0.82
C-1311	0.49 ± 0.09	0.83 ± 0.28
C-1330	4.51 ± 0.9	3.75 ± 1.9
C-1371	2.17 ± 0.39	2.83 ± 0.19
C-1415	2.48 ± 0.64	2.35 ± 0.39
C-1419	3.04 ± 0.59	3.23 ± 0.68
C-1492	2.13 ± 1.4	3.68 ± 0.43
C-1554	8.29 ± 2.6	5.02 ± 0.09
C-1558	1.70 ± 0.11	2.95 ± 0.77

[a] IC_{50} DNA and IC_{50} RNA are the concentrations of compounds inhibiting incorporation of [^{3}H]-labeled precursors into DNA or RNA, respectively, by 50%.

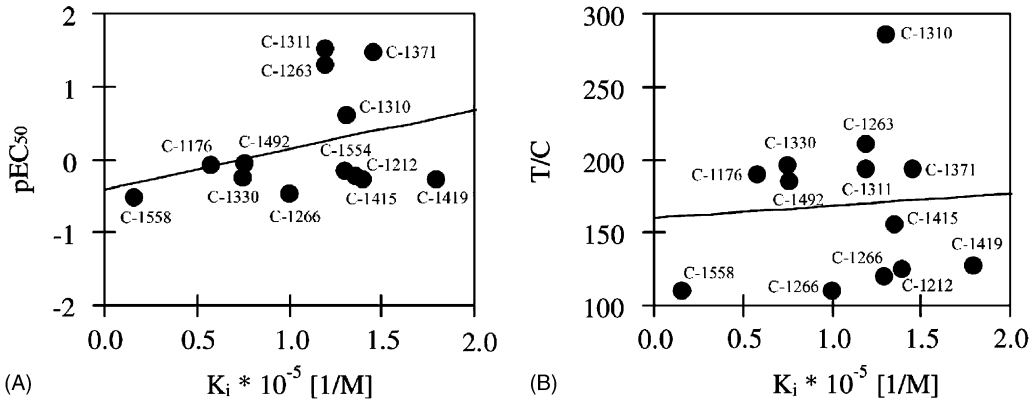

Fig. 5. Correlations between DNA binding affinity and biological activity of studied imidazoacridinones. (A) Cytotoxic activity (expressed as the negative logarithm from cytotoxic activity, pEC_{50}) vs. binding constant (K_i). (B) *In vivo* antitumor activity (*T*/*C*) vs. binding constant (K_i).

respectively) and drug cytotoxicity (pEC_{50} values, $R = 0.32$ and 0.19, respectively, $P > 0.05$) (Fig. 5 and data not shown). Likewise, there was no correlation between these DNA binding parameters and drug antitumor properties (*T*/*C* values, $R = 0.07$ and 0.52, respectively, $P > 0.05$). Finally, the correlation between drug binding properties and the ability to inhibit nucleic acid synthesis (expressed as IC_{50} values, Table 4) could not be found (data not shown).

4. Discussion

IA are a group of interesting anticancer agents and the lead compound, C-1311, is accepted for phase I clinical trials. Various observations suggested that DNA binding might be involved in the action of IA [4,7,8,22]. The ability to interact with DNA, in general, and specific binding properties such as: (a) mode of interactions, (b) affinity to DNA, (c) DNA duplex stabilization, and (d) kinetics of association/dissociation can influence biological effects of the drugs. This study systematically characterized and quantitated several of the mentioned attributes for a series of IA analogs. The results confirm the ability of IA to interact non-covalently with DNA and provide the evidences for their DNA intercalating potential. Crystallographic structure of C-1311 revealed that the acridinone core of this compound is planar (Fig. 1), similar to triazoloacridinone derivatives [23]. This acridinone moiety can be expected to be planar also in the structures of other IA compounds. All IA compounds examined were able to bind to DNA, and this interaction reflects drug intercalation between DNA base pairs, as directly evidenced for C-1311 by the DNA unwinding assay. Additionally, the average binding site size of 2–3 bp (Table 4), and fast kinetics of establishing and disruption of drug:DNA complexes (data not shown) are supportive of the intercalative mode of binding of IA to DNA.

The affinity of IA drugs to DNA, with binding constants, K_i, ranging from 0.16×10^5 to 1.46×10^5 M^{-1} (Table 4), is modest, similar to the binding affinity of various intercalating acridine derivatives [16,24]. Likewise, the ability of IA drugs to stabilize DNA duplexes is typical of acridines, with increases in 'melting' temperature of ctDNA, ΔT_m, ranging from 2.4 to 15.3° for drug:DNA molar ratio 1:4 (Table 4). The higher DNA affinity reported by others for C-1311 [7,22] in low salt buffer points to a role of electrostatic interactions, probably between positively charged side chains of IA and polyanionic DNA phosphate backbone [25].

Although DNA-binding properties of the studied drugs are qualitatively and quantitatively similar, they appear to be influenced by the position and the nature of the substituents in the acridine core. The presence of hydroxyl group in position 8 or 9 in acridinone ring slightly increases DNA affinity compared to unsubstituted- or alkyl-substituted derivatives, possibly due to additional hydrogen bonds with DNA phosphate backbone. As noted previously [1,2,26], IA with 8-OH group (C-1263, C-1310, C-1311, C-1371) were considerably more potent cell growth inhibitors than other derivatives. Similar structure–activity relationship is observed for the inhibition of nucleic acid synthesis. Relocation of OH group to position 9 drastically decreases biological activity, while DNA affinity is not affected (C-1311, 8-OH and C-1419, 9-OH).

Modeling studies suggest that the charged diaminoalkyl side chain of IA compounds can interact with DNA in the minor groove [27]. In addition to intercalation, such interaction is likely to further stabilize IA–DNA complexes. The influence of the diaminoalkyl side chain on drug affinity to DNA and biological properties is not clear. For compounds without 8-OH group, the increase in number of carbon atoms between nitrogen atoms from two to three (C-1176, two and C-1212, three carbons) raises DNA binding affinity and decreases cytotoxic activity. In the case of derivatives bearing 8-OH group, the increase in number of carbon atoms (C-1263, two and C-1371, three) augments cytotoxic activity whereas

somewhat decreases DNA affinity. Further increase in side chain length (C-1266 and C-1492, five carbon atoms) significantly reduces cytotoxic and antitumor activity.

In general, among tested compounds there is no clear-cut correlation between any of the examined parameters of drug binding to naked DNA and inhibitory activities measured in intact cells. The interpretation of this lack of correlation is not straightforward given the profound differences between naked DNA vs. intact cell systems and the likely contributions of other factors, starting with cellular drug uptake. In depth studies with related classes of intercalating drugs, such as anthracenediones [28], aza-anthracenediones [29], 1-nitroacridine derivatives [16] or anthracyclines [30] repeatedly showed poor correlation between drug cytotoxic potency and DNA binding affinities. In several of such cases, further studies revealed drug metabolic activation in cellular systems, leading to the formation of covalent DNA adducts [31,32]. Our recent studies indicate that this can be also the case with the IA drugs [33]. In that context, the intercalative properties of IA drugs may help position drug molecules on DNA for the covalent reaction, but *per se*, may not be sufficient to account for the differences in their biological activities.

In conclusion, our results demonstrate that DNA intercalation may be a component of the mechanism of action of C-1311 and related IA. However, in addition to their intercalative binding, other factors seem to be required for the prominent cytotoxic and antitumor activities of imidazoacridinone drugs. Studies are under way to systematically evaluate cellular effects of C-1311 and related IA that may identify drug growth inhibitory properties in addition to intercalative DNA binding.

Acknowledgments

We are grateful to Dr. Jan M. Woynarowski (Institute for Drug Development, San Antonio, TX) for helpful discussions and critical reading of this manuscript, and to Dr. Jan Kapuścinski (University of Gdańsk, Poland) for his invaluable methodological suggestions. This work was supported in part by the Polish National Committee for Scientific Research (KBN), Grant no. 4PO5F 00612.

References

[1] Cholody WM, Martelli S, Paradziej-Lukowicz J, Konopa J. 5-(aminoalkyl)amino]imidazo[4,5,1-de]acridin-6-ones as a novel class of antineoplastic agents. Synthesis and biological activity. J Med Chem 1990;33:49–52.

[2] Cholody WM, Martelli S, Konopa J. Chromophore-modified antineoplastic imidazoacridinones. Synthesis and activity against murine leukemias. J Med Chem 1992;35:378–82.

[3] Kusnierczyk H, Cholody WM, Paradziej-Lukowicz J, Radzikowski C, Konopa J. Experimental antitumor activity and toxicity of the selected triazolo- and imidazoacridinones. Arch Immunol Therap Exp 1994;42:415–23.

[4] Burger AM, Double JA, Konopa J, Bibby MC. Preclinical evaluation of novel imidazoacridinone derivatives with potent activity against experimental colorectal cancer. Br J Cancer 1996;74:1369–74.

[5] Mazerska Z, Augustin E, Składanowski A, Bibby MC, Double JA, Konopa J. C-1311. Drugs Fut 1998;23:702–6.

[6] Składanowski A, Plisov SY, Konopa J, Larsen AK. Inhibition of DNA topoisomerase II by imidazoacridinones, new antineoplastic agents with strong activity against solid tumors. Mol Pharmacol 1996;49:772–80.

[7] Burger AM, Jenkins TC, Double JA, Bibby MC. Cellular uptake, cytotoxicity and DNA binding studies of the novel imidazoacridinone antineoplastic agent C-1311. Br J Cancer 1999;81:367–75.

[8] Dzięgielewski J, Składanowski A, Konopa J. Noncovalent binding of potent imidazoacridinones to DNA. Ann Oncol 1996;7(Suppl 1):56.

[9] Augustin E, Wheatley DN, Lamb J, Konopa J. Imidazoacridinones arrest cell-cycle progression in the G_2 phase of L1210 cells. Cancer Chemother Pharmacol 1996;38:39–44.

[10] Sheldrick GM. Phase annealing in SHELX-90 direct methods for larger structures. Acta Cryst A 1990;46:467–73.

[11] Sheldrick GM, SHELXL-97. Program for the solution and the refinement of crystal structures. University of Gőttingen, Gőttingen, 1997.

[12] Schwarz G, Klose S, Balthasar W. Cooperative binding to linear biopolymers. 2. Thermodynamic analysis of the proflavine-poly(L-glutamic acid) system. Eur J Biochem 1970;12:454–60.

[13] Kapuscinski J, Darzynkiewicz Z. Interactions of antitumor agents ametantrone and mitoxantrone (novatrone) with double-stranded DNA. Biochem Pharmacol 1985;34:4203–13.

[14] Pachter JA, Huang CH, DuVernay Jr. VH, Prestayko AW, Crooke ST. Viscometric and fluorometric studies of deoxyribonucleic acid interactions of several new anthracyclines. Biochemistry 1982;21:1541–7.

[15] McGhee JD, von Hippel PH. Theoretical aspects of DNA–protein interactions: co-operative and non-co-operative binding of large ligands to a one-dimensional homogeneous lattice. J Mol Biol 1974;86:469–89.

[16] Pawlak K, Matuszkiewicz A, Pawlak JW, Konopa J. The mode of action of cytotoxic and antitumor 1-nitroacridines. I. The 1-nitroacridines do not exert their cytotoxic effects by physicochemical binding with DNA. Chem Biol Interact 1983;43:131–49.

[17] Pommier Y, Covey JM, Kerrigan D, Markovits J, Pham R. DNA unwinding and inhibition of mouse leukemia L1210 DNA topoisomerase I by intercalators. Nucleic Acids Res 1987;15:6713–31.

[18] Składanowski A, Konopa J. Adriamycin and daunomycin induce programmed cell death (apoptosis) in tumor cells. Biochem Pharmacol 1993;46:375–82.

[19] Lown JW, Hanstock CC. High field ^{1}H NMR analysis of the 1:1 intercalation complex of the antitumor agent mitoxantrone and the DNA duplex [d(CpGpCpG)]. J Biomol Struct Dynam 1985;2:1097–106.

[20] de Isabella P, Palumbo M, Sissi C, Capranico G, Carenini N, Menta E, Oliva A, Spinelli S, Krapcho AP, Giuliani FC, et al. Topoisomerase II DNA cleavage stimulation, DNA binding activity, cytotoxicity, and physico-chemical properties of 2-aza- and 2-aza-oxide-anthracenedione derivatives. Mol Pharmacol 1995;48:30–8.

[21] Delbarre A, Roques BP, Le Pecq JB, Lallemand JY, Nguyen-Dat-Xuong. PMR studies of the self-association of DNA intercalating ellipticine derivatives in aqueous solution. Biophys Chem 1976:4;275–9.

[22] Berger B, Marguardt H, Westendorf J. Pharmacological and toxicological aspects of new imidazoacridinone antitumor agents. Cancer Res 1996;56:2094–104.

[23] Arjunan P, Arora SK, Cholody WM. Structural studies on DNA binding drugs: crystal structure and molecular dynamics studies of triazoloacridinones. Acta Crystallogr B 1993;49:96–101.
[24] Denny WA, Twigden SJ, Baguley BC. Steric constraints for DNA binding and biological activity in the amsacrine series. Anti-Cancer Drug Des 1986;1:125–32.
[25] Chaires JB, Satyanarayana S, Suh D, Fokt I, Przewloka T, Priebe W. Parsing the free energy of anthracycline antibiotic binding to DNA. Biochemistry 1996;35:2047–53.
[26] Mazerska Z, Augustin E, Dzięgielewski J, Cholody WM, Konopa J. QSAR of acridines. III. Structure–activity relationship for antitumor imidazoacridinones and intercorrelations between *in vivo* and *in vitro* tests. Anti-Cancer Drug Des 1996;11:73–88.
[27] Mazerski J, Muchewicz K. The intercalation of imidazoacridinones into DNA induces conformational changes in their side chain. Acta Biochim Pol 2000;47:65–78.
[28] Johnson RK, Zee-Cheng RK, Lee WW, Acton EM, Henry DW, Cheng CC. Experimental antitumor activity of aminoanthraquinones. Cancer Treat Rep 1979;63:425–39.
[29] Hazlehurst LA, Krapcho AP, Hacker MP. Correlation of DNA reactivity and cytotoxicity of a new class of anticancer agents: aza-anthracenediones. Cancer Lett 1995;91:115–24.
[30] Capranico G, Zunino F, Kohn KW, Pommier Y. Sequence-selective topoisomerase II inhibition by anthracycline derivatives in SV40 DNA: relationship with DNA binding affinity and cytotoxicity. Biochemistry 1990;29:562–9.
[31] Pawlak K, Pawlak JW, Konopa J. Cytotoxic and antitumor activity of 1-nitroacridines as an aftereffect of their interstrand DNA cross-linking. Cancer Res 1984;44:4289–96.
[32] Składanowski A, Konopa J. Relevance of interstrand DNA cross-linking induced by anthracyclines for their biological activity. Biochem Pharmacol 1994;47:2279–87.
[33] Mazerska Z, Dzięgielewski J, Konopa J. Enzymatic activation of a new antitumor drug, 5-diethylaminoethylamino-8-hydroxyimidazoacridinone, C-1311, observed after its intercalation into DNA. Biochem Pharmacol 2001;61:685–94.